Article

Effect of Short Term Water Exposure on the Mechanical Properties of Halloysite Nanotubes-Multi Layer Graphene Reinforced Polyester Nanocomposites

Mohd Shahneel Saharudin [1,2,*], Rasheed Atif [2] and Fawad Inam [2]

[1] Universiti Kuala Lumpur Institute of Product Design and Manufacturing (UniKL IPROM), Cheras, Kuala Lumpur 56100, Malaysia

[2] Department of Mechanical and Construction Engineering, Faculty of Engineering and Environment, Northumbria University, Newcastle upon Tyne NE1 8ST, UK; aatif.rasheed@northumbria.ac.uk (R.A.); fawad.inam@northumbria.ac.uk (F.I.)

* Correspondence: mohd.saharudin@northumbria.ac.uk

Abstract: The influence of short term water absorption on the mechanical properties of halloysite nanotubes-multi layer graphene reinforced polyester hybrid nanocomposites has been investigated. The addition of nano-fillers significantly increased the flexural strength; tensile strength and impact strength in dry and wet conditions. After short term water exposure; the maximum microhardness; tensile; flexural and impact toughness values were observed at 0.1 wt% MLG. The microhardness increased up to 50.3%; tensile strength increased up to 40% and flexural strength increased up to 44%. Compared to dry samples; the fracture toughness and surface roughness of all types of produced nanocomposites were increased that may be attributed to plasticization effect. Scanning electron microscopy revealed that the main failure mechanism is caused by the weakening of nano-filler-matrix interface induced by water absorption. It was further observed that synergistic effects were not effective at concentration of 0.1 wt% to produce considerable improvement in mechanical properties of produced hybrid nanocomposites.

Keywords: nanocomposites; halloysite nanotubes; multi-layer graphene; water absorption; mechanical properties

1. Introduction

In recent years, composite materials have been widely used to replace, with advantage, not only steel but even light alloys in the construction of various components and structures such as wind turbine blades, aircraft, automobile, sporting goods, civil and marine structures [1]. Unsaturated polyester resins are the most commonly used thermosetting system due to their low cost factor and versatility to be altered into enormous composite fabrications [2,3].

Polyester is an excellent matrix for composites because of its many features superior to that of the competition, including but not limited to handling characteristics, improvement in composite mechanical properties, acceptable cost and processing flexibility [4]. Albeit polyester resins are extensively used as a matrix in polymer composites, curing of these resins results in brittleness due to their high cross linking level [5].

During service, polymeric materials are exposed to a variety of environmental conditions such as moisture, solvents, oil, temperature, mechanical loads and radiation [6,7]. In particular, all polymer composites absorb moisture and the water molecules can act as a plasticizer by influencing simultaneously the fibres, the matrix and the interface, thus creating regions of poor transfer efficiency, which results in a reduction of mechanical properties [8–10]. Several factors are known to affect the way in which composite materials absorb water [8,11], such as temperature, fibre volume fraction, reinforcement architecture, fibre nature (permeable or impermeable), area of exposed surfaces, polarity of the molecular structure, degree of cross- linking and degree of crystallinity [10].

A wide range of engineering properties can be improved with a low level of halloysite nanotubes typically less than 5 wt% [12]. In our previous work, we studied the tensile properties of polyester nanocomposites reinforced with halloysite nanotubes. We found that the incorporation of halloysite nanotubes increased Young's modulus up to 70% compared to unfilled polyester exposed to diluted methanol [13]. Tensile strength and impact toughness increased 17.4% and 184% respectively [13]. Other improved physical and engineering properties include fire retardancy [14,15], barrier resistance [16] and ion conductivity [12]. Another advantage of clay nanocomposites is that the optical properties of the polymer are not considerably affected. This property is very useful for medical applications where optical clarity is vital such as catheter connectors, cardiac surgery products and intravenous infusion components [17,18]. Alamri and Low studied the effect of water on the mechanical properties of halloysite nanotubes-reinforced epoxy. They observed that the incorporation of halloysite nanotubes was able to reduce water absorption and improve mechanical properties of the nanocomposites after water immersion [19].

Graphene-based polymer composites show superior mechanical, thermal, gas barrier, electrical and flame retardant properties, compared to the neat polymer [20–22]. One reason that graphene research has progressed so fast is that the laboratory procedures enabling us to obtain high-quality graphene are relatively simple and economical [23]. Apart from that, graphene based materials has been used is different fields such as composites and coatings, electronics devices, energy storage, sensors and biomedical applications [20]. Atif et al. in their study reported that MLG improved Young's modulus and microhardness by 25.7% and 18.3%, respectively [24]. The MLG also increased T_g and storage modulus compared to unfilled epoxy [25–27].

In this work, the effect of short term water absorption on the mechanical properties of polyester based nanocomposites reinforced with halloysite nanotubes (HNT), multi-layer graphene (MLG) and HNT-MLG (hybrid fillers) has been studied. The influence of HNT, MLG and HNT-MLG has been tested in terms of weight gain of nanocomposites due to water absorption. The effect of nano-filler addition on improving polyester matrix mechanical properties in dry and wet condition has been investigated.

The knowledge of the effects of moisture absorption and high temperature exposure on flexural, tensile and impact properties behaviour is not easily found in literature for hybrid polyester composites reinforced with HNT and MLG. This appears to be important with a view to broadening the industrial applications of these nano-composites in particular with reference to coating industry. The aim of making hybrid nanocomposites was to study whether synergistic effects can reduce the water degradation effect caused by water absorption at low weight fraction of 0.1 wt %.

2. Materials and Methods

HNT (Figure 1(a)) was used as reinforcement filler and acquired from Sigma Aldrich. The diameter of HNT was between 30-70 nm with length 1-4 μm. It had a tube-like morphology with density of 2.53 g/cm^3 and surface area 64 m^2/g. HNT has low electrical and thermal conductivities and strong hydrogen interactions. The tubular morphology, high aspect ratio, and low percolation make HNT a prospective reinforcement for polyester and other polymers.

MLG (Figure 1(b)) of 12 nm average thickness and 4.5 μm average lateral size with surface area of 80 m^2/g was used as second filler purchased from Graphene Supermarket. The polyester resin of the NORSODYNE O 12335 AL was acquired from East Coast Fibreglass, UK. The resin had density of 1.2 g/cm^3. The catalyst (hardener) was methyl ethyl ketone peroxide solution in dimethyl phthalate and purchased from East Coast Fibreglass, UK.

To produce monolithic polyester samples, the resin (Norsodyne O 12335 Al) was mixed with catalyst (Butanox M-50) in a polyester: catalyst ratio of 98:2. Following thorough hand mixing for 10 min, vacuum degassing was again carried out for 10 minutes. The resin was poured into silicone moulds (without any release agent) and cured at room temperature for 24 h followed by post-curing at 80 ^{o}C for 2 hours to ensure completion of the crosslinking [5,28]. In this research, four different samples were produced; monolithic polyester, 0.05 wt% HNT-0.05 wt% MLG, 0.1 wt% HNT and 0.1 wt% MLG.

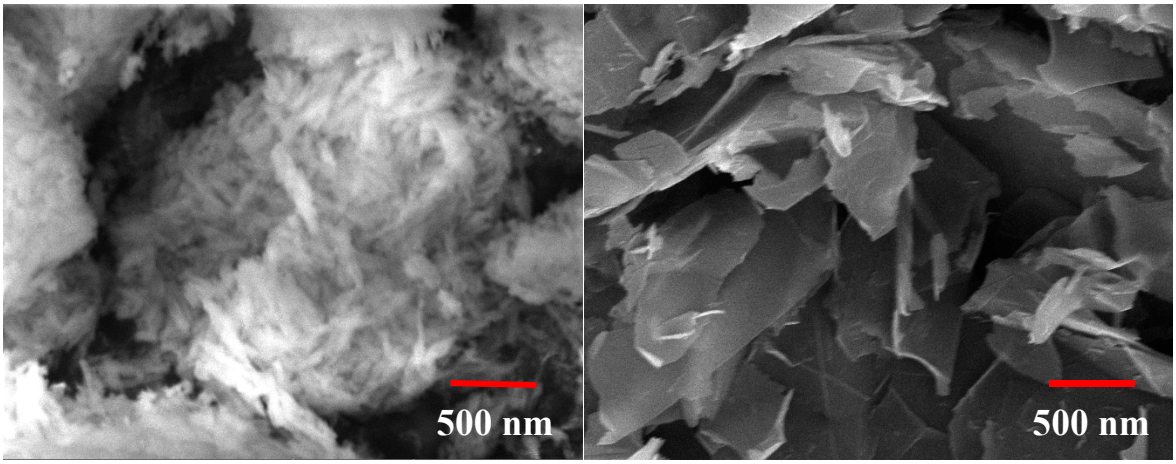

(a) (b)

Figure 1. SEM images: (a) HNT, and (b) MLG.

3. Characterisation

DMA (Model 8000, Perkin-Elmer) was used to determine dynamic storage modulus (E′), and loss modulus (E′′) of the samples. The loss factor tanδ was calculated as the ratio (E′′/E′). Rectangular test specimens of dimensions 20 x 5 x 3 mm were used with a single cantilever clamp. All tests were carried out by temperature sweep method (temperature ramp from 30 °C to 130 °C at 5 °C/min) at a constant frequency of 1 Hz. The maximum force of DMA was 10 N and applied during all DMA tests. The glass transition temperature (T_g) was taken as the temperature value at the peak of tanδ curves. The densification of samples was calculated according to ASTM D792. The densities of polyester, hardener, HNT and water were 1.2, 1.18, 2.53 and 0.9975 g/cm^3, respectively. The following equations were used to obtain the experimental density and densification.

$$Experimental\ density = \frac{weight\ in\ air}{weight\ in\ air - weight\ in\ water}\ x\ density\ of\ water \qquad \text{Equation (1)}$$

$$Densification\ (\%) = \frac{experimental\ density}{theoretical\ density}\ x\ 100 \qquad \text{Equation (2)}$$

To measure water absorption, rectangular specimens with dimensions 80 x 10 x 4 mm were immersed into the liquid media at room temperature. Before weighing procedure, any retained water was removed from its surface with an absorbent paper. The water absorption in the sample was measured as % weight increase in the samples. Equation 3 was used to calculate the water absorption in the specimens.

$$W_c = (W_t - W_o)\ x\ 100/W_o \qquad \text{Equation (3)}$$

Where W_t is the weight of specimen at time t (i.e. after immersion in the liquid) and W_o is the initial weight of the sample, i.e. before placing in water. Light transmittance in the UV-visible spectroscopy (Shimadzu UV-2600) was used to quantify the dispersion of fillers in polyester system. Tests were carried out on both dry and wet samples. Light transmittance of nano-filler dispersions in polyester was recorded at wavelength between 400-1400 nm. Five specimens of dimensions 80 x 10 x 3 mm were tested for each set of conditions. The optical transmittance graphs for dry and wet samples are also presented.

The effect of water absorption on the mechanical properties of HNT-polyester nanocomposites was investigated after placing the specimens in water for 24 h at 60 °C and compared with the same nanocomposites in dry condition (without immersion in water). Vickers microhardness test was performed using the Buehler Micromet II for the monolithic polyester and its nanocomposites. The load applied was 200 g for 10 seconds. After water immersion, the samples were taken out and the liquid completely wiped out from the specimen surface.

Tensile test and three-point bend (Figure 2 (a) and (b)) tests were performed using Instron Universal Testing Machine (Model 3382). Five specimens were tested for each composition. The displacement rate for three-point bend and tensile tests were kept 1 mm/min. Tensile test properties

Preprints (www.preprints.org) | NOT PEER-REVIEWED | Posted: 5 January 2017 doi:10.20944/preprints201701.0024.v1

Peer-reviewed version available at Polymers 2017, 9, 27; doi:10.3390/polym9010027

were carried out according to ISO 527 (Figure 2(a)) with specimen thickness of 3 mm. Three-point bending test was performed according to ISO 178 with dimensions 80 x 10 x 4 mm (Figure 2(b)). Charpy impact toughness test was performed according to ASTM D6110 (Figure 2(c)) using notch samples. A notch of (45°) was made in the centre of samples. The impact toughness was obtained using equation (4), where m is mass of hammer (kg), g is standard gravity (9.81 m/s²), h is the length of hammer (m) and t is sample thickness (mm).

$$Impact\ toughness = \frac{mgh\ (\cos\beta - \cos\alpha)}{wt} \quad \text{Equation (4)}$$

Instron Universal Testing Machine was also used to perform fracture toughness tests. The fracture toughness (K_{1C}) was determined using a single edge notch three-point bending (SEN-TPB) specimen (ASTM D5045) as shown in Figure 2(d). The displacement rate used was 1mm/min. The dimensions were 3 x 6 x 36 mm with a crack length of 3 mm at the mid of sample. K_{1C} was calculated using linear fracture mechanics by following relationship,

$$K_{IC} = \frac{P_{max}(\frac{a}{w})}{BW^{1/2}} \quad \text{Equation (5)}$$

Where $f(a/W)$ is the calibration factor for the samples which is given as:

$$f(\frac{a}{w}) = \frac{[(2+\frac{a}{w})\{0.0866+4.64(\frac{a}{w})^2+14.72(\frac{a}{w})^3-5.6(\frac{a}{w})^4\}]}{(1-\frac{a}{w})^{3/2}} \quad \text{Equation (6)}$$

An Alicona optical microscope was used to study the topographical features of produced samples. The Alicona Infinite Focus optical microscope (G4, Alicona, Raaba/Graz, Austria) was used to generate optical micrographs and measure topographical features. The Alicona optical microscope is a non-contact method (focus-follow method) for topography measurement.

Scanning Electron Microscopy (SEM) analysis using a FEI Quanta 200, was carried out of the fractured surfaces of tensile specimens to evaluate the fracture modes in the samples. The fractured portions were cut from the specimens and a layer of gold was applied using Emscope sputter coater model SC500A.

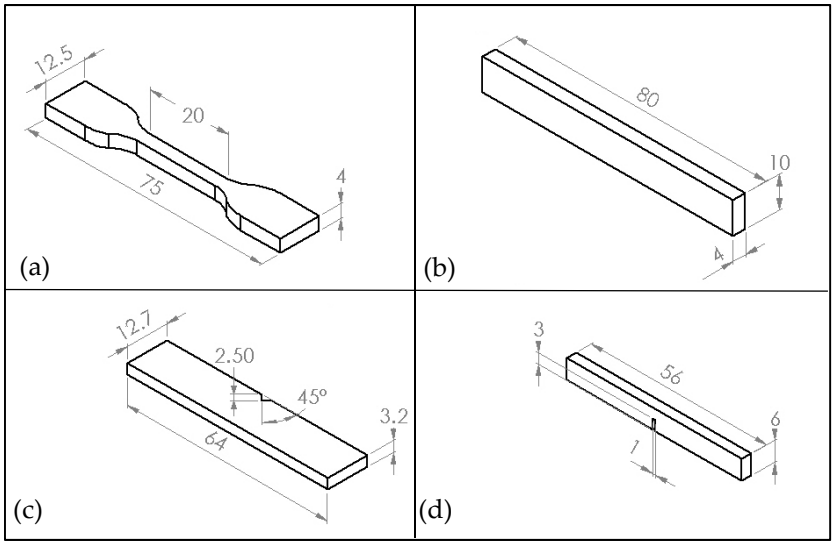

Figure 2. The illustration of specimens: (a) tensile, (b) flexural, (c) Charpy impact toughness, and (d) fracture toughness, K_{1C}.

4. Results

In this research, the addition of 0.1 wt% of HNT and MLG increased the T_g as shown in Figure 3. An increase in T_g with HNT and MLG shows that the fillers were uniformly dispersed [7,26]. As for HNT, the change in T_g associated with inorganic fillers was reported and proposed by others [29]. The two common factors were rigid phase reinforcement and destroying epoxy based polymer network structure [30]. Other authors also proposed that HNT and other clay particles restrict the mobility of polymer chains [31,32]. In case of MLG, when it is uniformly dispersed, the wrinkled texture and high surface area influence the maximum exothermic heat flow temperature by restricting polymer chain mobility thereby causing an increase in T_g [27].

In dry condition, monolithic polyester (MP) recorded the lowest value of T_g with 77.9 °C. The T_g increased to 78.3 °C for HNT-MLG polyester nanocomposites and increased to 80.4 °C in case of 0.1 wt% HNT reinforced polyester. The maximum T_g was in case of 0.1 wt% MLG reinforced polyester with 82.6 °C (6% increase). After water exposure, the T_g decreased for all nanocomposites (compared to dry nanocomposites system). The lowest T_g was observed for MP as T_g dropped from 77.9 °C to 70 °C. The highest T_g was observed for 0.1 wt% MLG reinforced polyester (77.34 °C). The lowering of T_g is an evidence of plasticization effect by water [33]. Moisture wicking along the fiber-matrix interface degrades the interfacial bond strength, resulting in loss of micro-structural integrity [33]. The storage modulus of nanocomposites for dry samples is shown in Figure 4(a). The increase of storage modulus during glass transition temperature can be associated with the decrease in polymeric chain mobility [34] and enhancement of stiffness [35]. In case of 0.1 wt% HNT and 0.1 wt% MLG show significant improvement of storage modulus particularly at lower temperature. The maximum storage modulus at 40 °C was recorded for MLG filler. The storage modulus for all reinforced polyester later decreased as they approached the glass transition temperature (T_g). It can be observed that storage modulus increased while loss modulus decreased for hybrid (0.05 wt% HNT-0.05 wt% MLG), 0.1 wt% HNT and 0.1 wt% MLG reinforced polyester compared with monolithic polyester. The storage modulus for nanocomposites exposed to water is shown in Figure 4 (b). It can be seen the storage modulus and loss modulus (Figure 5) considerably decreased as a result of matrix softening [36].

The optical transmittance of the nanocomposites was investigated. In Figure 6 (a) and (b), it can be observed that MP is essentially highly transparent over the 400-1400 nm wavelength. The average transmittance value of MP is 72.9%. At 0.1 wt% HNT, it recorded 57.6% average value. The 0.05 wt% HNT-0.05 wt% MLG reinforced polyester recorded only 4.3% optical transmittance. The 0.1 wt% MLG had an optical transmittance of 0.29%. It can be seen, even at 0.05 wt% HNT-0.05 wt% MLG, that the optical transmittance dropped significantly. After water exposure, similar trend was observed where monolithic polyester had the highest optical transmittance. However, the water exposure significantly reduced the optical transmittance for monolithic polyester (decrease of 46.3% compared to dry condition). The 0.1 wt% HNT reinforced polyester lost 37% of optical transmittance due to water absorption. The optical transmittance for 0.05 wt% HNT-0.05 wt% MLG reinforced polyester and 0.1 wt% MLG reinforced polyester were also found to be decreased but the values were not significant.

The densification of samples versus type of reinforcement is shown in Figure 7(a). The large standard deviations for monolithic polyester indicate porosity within the samples. That shows air entrapment during processing [37]. Another reason for this could be the quick curing of polyester resin as the volatiles could not escape during curing [38,39]. The casting technique used on the other hand is not usually considered 100% reproducible like latex technology [40]. The water absorption test is shown in Figure 7(b). It can be seen the monolithic polyester absorbed more water than other nanocomposites system. For 0.05 wt% HNT-0.05 wt% MLG reinforced polyester recorded water absorption of 1.42%. The 0.1 wt% HNT reinforced polyester recorded 1.35% and 0.1 wt% MLG reinforced polyester with 1.2% of water absorption.

The microhardness result is shown in Figure 7(c). Compared to monolithic polyester, the 0.05 wt% HNT-0.05 wt% MLG reinforced polyester improved the microhardness from 177 HV to 221 HV (25% increase). The microhardness increased steadily in case of 0.1 wt% HNT (49% increase) and 0.1 wt% MLG (50.3% increase). After water exposure, the monolithic polyester recorded only 111 HV. The microhardness for nanocomposites exposed to water improved in case of 0.05 wt% HNT-MLG, 0.1 wt% HNT and 0.1 wt% MLG, however, the values were lower than those in dry conditions. The reduction of microhardness was caused by the surface softening of polyester matrix by water [41,42]. Flexural modulus of the nanocomposites is shown in Figure 7(d). For dry samples, the maximum flexural modulus was observed in case of 0.1 wt% MLG (60.6% increase) followed by 0.1 wt% HNT (increase 50.6%). For samples exposed in water, the similar trend was observed. The maximum flexural modulus was recorded in case of 0.1 wt% MLG. The flexural modulus increased from 0.62 GPa to 1.15 GPa (increase 85.5%).

Preprints (www.preprints.org) | NOT PEER-REVIEWED | Posted: 5 January 2017 doi:10.20944/preprints201701.0024.v1

Peer-reviewed version available at Polymers 2017, 9, 27; doi:10.3390/polym9010027

Flexural strength of nanocomposites in dry and wet condition is presented in Figure 7(e). Minimum flexural strength was recorded in case of MP. The maximum flexural strength was observed in case of 0.1 wt% MLG reinforced polyester. The flexural strength increased from 55.7 MPa to 71.9 MPa (29% increase). After water exposure, the flexural strength showed degradation compared to unexposed samples. The lowest flexural strength was observed for MP with only 45 MPa. The flexural strength then steadily increased in case of 0.05 wt% HNT-0.05 wt% MLG (47 MPa), 0.1 wt% HNT (63 MPa) and 0.1 wt% MLG (65 MPa).

The variation in flexural strain of nanocomposites for dry and wet conditions is shown in Figure 7(f). In comparison with MP, the flexural strain decreased with the incorporation of nano-fillers. The increase in strength and stiffness reduced the flexural strain. After water exposure, the flexural strain increased for all samples. This could be due to the fact that water fill the gaps between the fillers and polymer matrix eventually lead to a decrease in flexural strength [43]. The water absorption leads to increase of plastic zone ahead of crack hence increase the flexural strain of all nanocomposites [44].

The variation of Young's modulus is shown in Figure 7(g). Monolithic polyester obtained 0.75 GPa of Young's modulus. The Young's modulus increased 7% in case of 0.1 wt% HNT. The highest Young's modulus was obtained for 0.1 wt% MLG reinforcement with an improvement of 60%. After water exposure, 0.1 wt% of MLG reinforcement also recorded the highest Young's modulus with an increase of 98% compared to MP. The variation in tensile strength is shown in Figure (h). At 0.1 wt% MLG reinforcement, the highest tensile strength was observed. The tensile strength increased from 32.4 MPa up to 47.3 MPa (46% increase) for dry samples. As for wet samples, the tensile strength increase from 28.3 MPa to 39.5 MPa. The tensile strain graph is shown in Figure 7(i). In dry condition, the tensile strain tend to have lower value than samples exposed in water environment. Dry samples were more stiff and have higher strength than samples tested after water exposure.

The variation of impact toughness is shown in Figure 7(j). For dry samples, MP recorded a value of 0.78 kJ/m^2. In case of 0.05 wt% HNT-0.05 wt% MLG, the impact toughness increased to 1 kJ/m^2. Further increase of impact toughness also can be seen for samples reinforced with 0.1 wt% HNT (1.4 kJ/m^2). The maximum increase of impact toughness was seen for samples reinforced with 0.1 wt% MLG (1.6 kJ/m^2). The fracture toughness (K_{1C}) is shown in Figure (k). The maximum fracture toughness was observed in case 0.1 wt% MLG reinforcement. The fracture toughness of this polyester system has been enhanced with the addition of 0.05 wt% HNT-0.05 wt% MLG, 0.1 wt% HNT and 0.1 wt% MLG. The fracture toughness increased from 0.3 MPa.m$^{1/2}$ to 0.6 MPa.m$^{1/2}$ (100% increase). In general, the water exposure increased the fracture toughness of the nanocomposites. Polyester reinforced with 0.1 wt% MLG recorded the highest fracture toughness. The fracture toughness increased from 0.48 MPa.m$^{1/2}$ to 0.8 MPa.m$^{1/2}$ (67% increase).

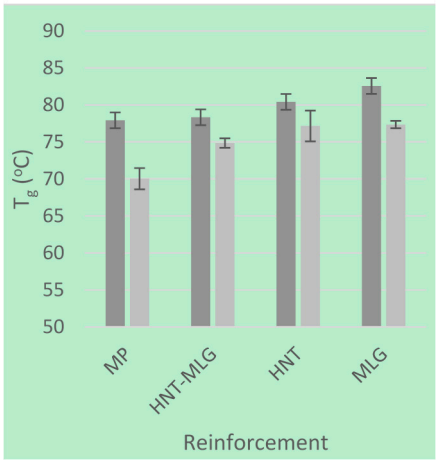

Figure 3. *Tg* of nanocomposites in dry condition and after water exposure

Preprints (www.preprints.org) | NOT PEER-REVIEWED | Posted: 5 January 2017 doi:10.20944/preprints201701.0024.v1

Peer-reviewed version available at Polymers 2017, 9, 27; doi:10.3390/polym9010027

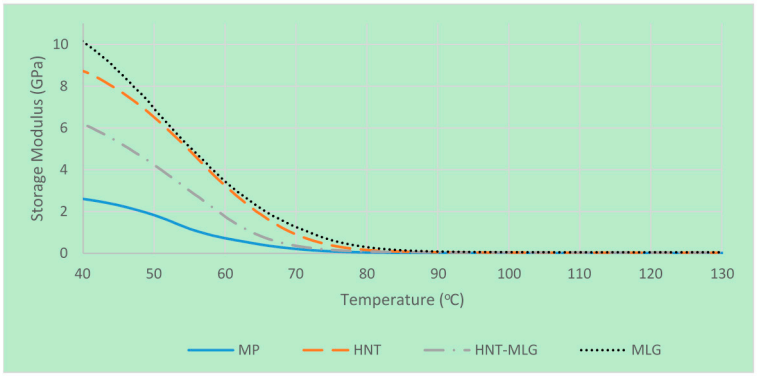

(a)

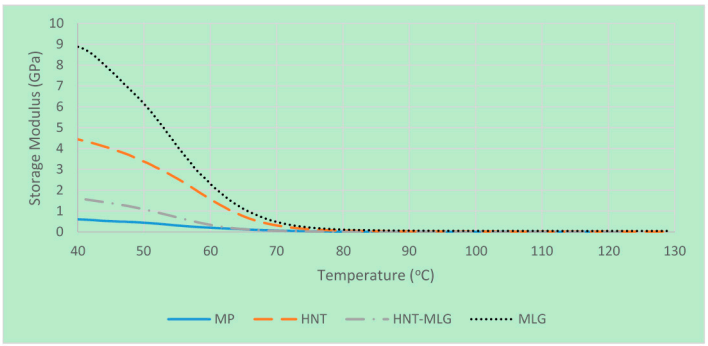

(b)

Figure 4. Storage modulus of nanocomposites in dry and after water exposure

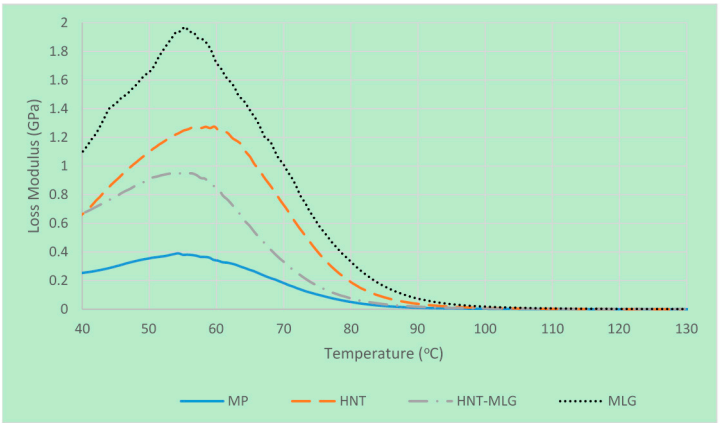

(a)

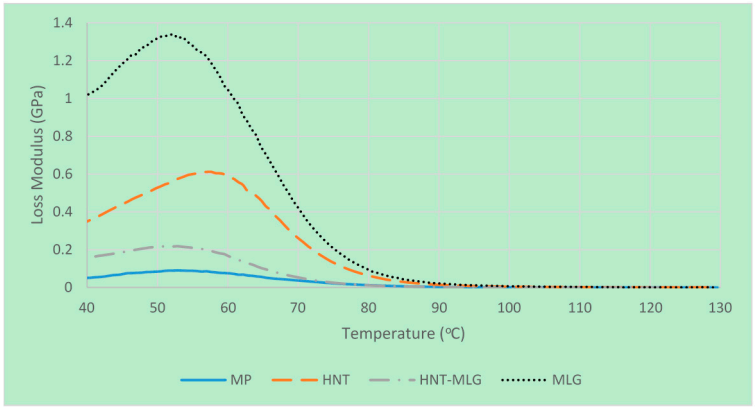

(b)

Figure 5. Loss modulus of nanocomposites in dry condition and after water exposure

Preprints (www.preprints.org) | NOT PEER-REVIEWED | Posted: 5 January 2017 doi:10.20944/preprints201701.0024.v1

Peer-reviewed version available at Polymers 2017, 9, 27; doi:10.3390/polym9010027

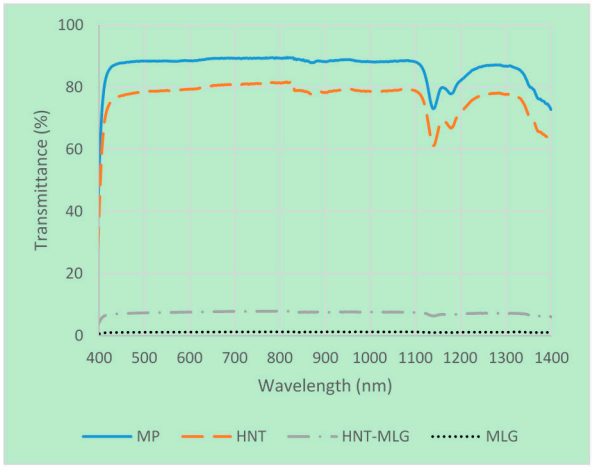

(a)

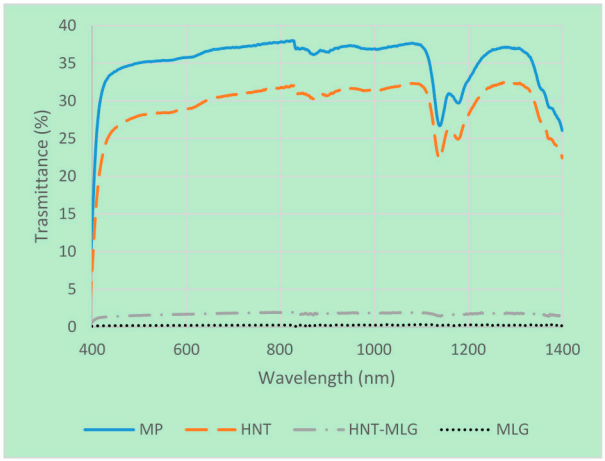

(b)

Figure 6. Optical transmittance of nanocomposites for dry (a) and after water exposure (b)

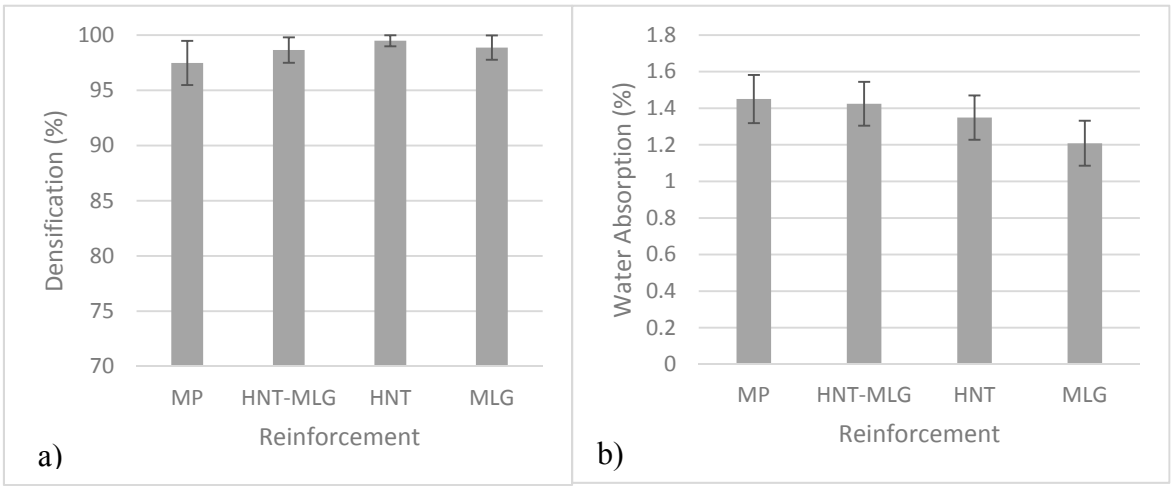

Preprints (www.preprints.org) | NOT PEER-REVIEWED | Posted: 5 January 2017 doi:10.20944/preprints201701.0024.v1

Peer-reviewed version available at Polymers 2017, 9, 27; doi:10.3390/polym9010027

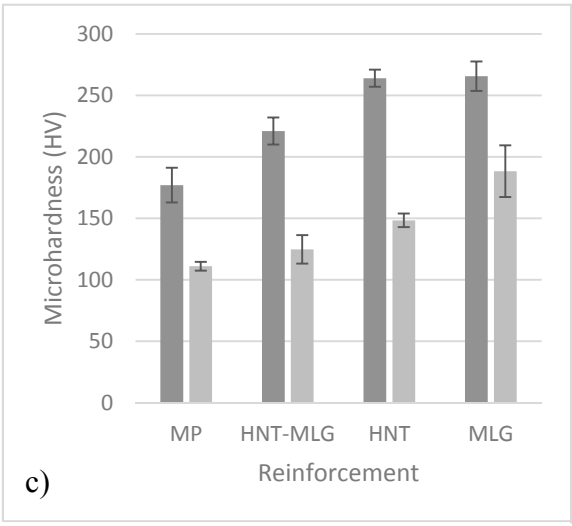

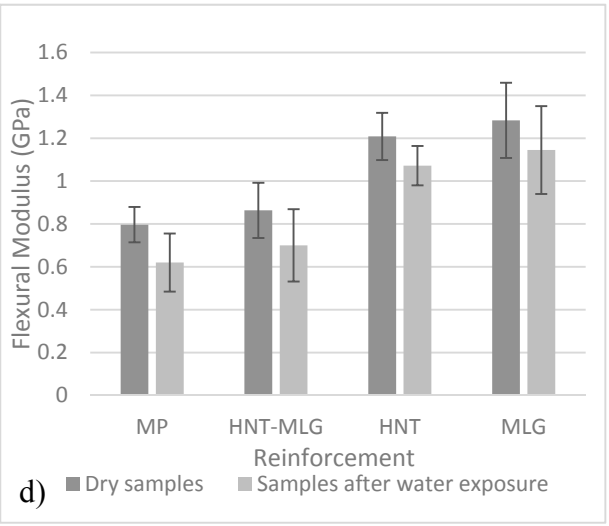

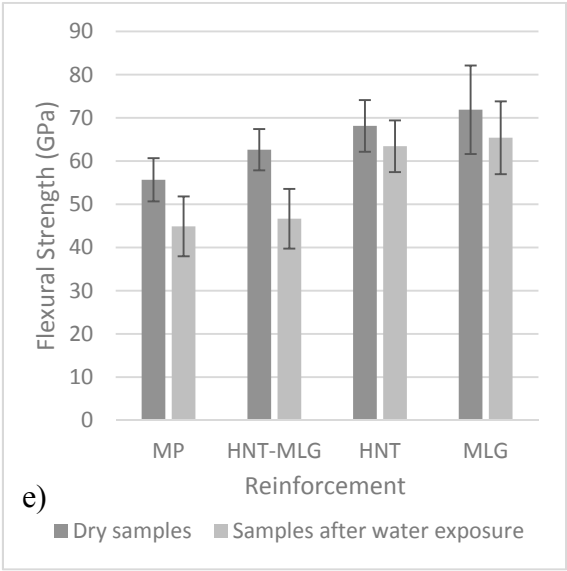

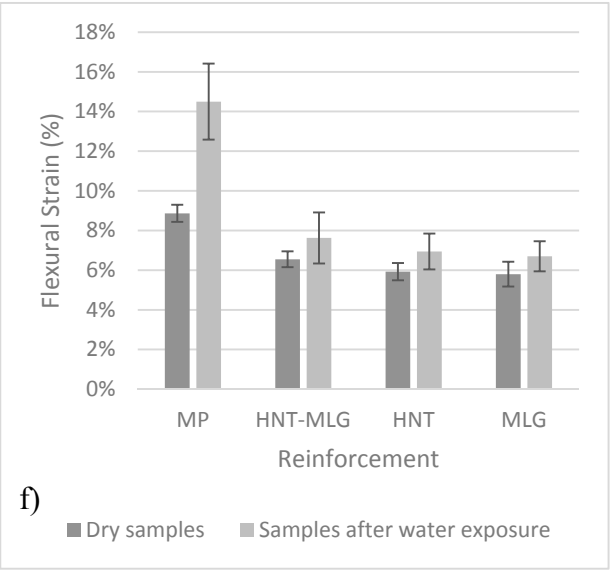

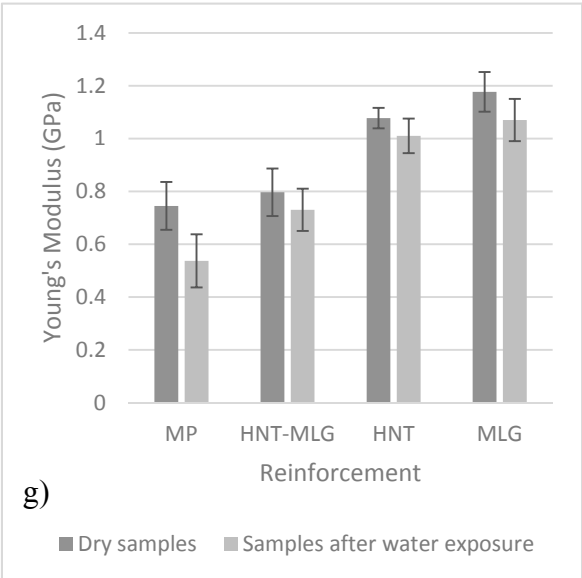

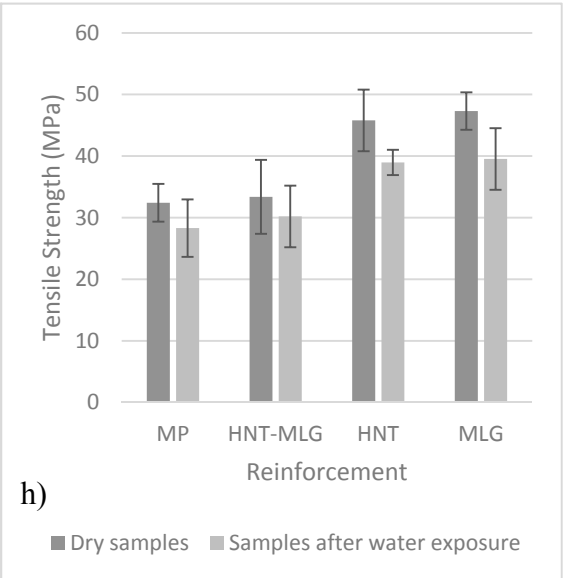

Preprints (www.preprints.org) | NOT PEER-REVIEWED | Posted: 5 January 2017 doi:10.20944/preprints201701.0024.v1

Peer-reviewed version available at Polymers 2017, 9, 27; doi:10.3390/polym9010027

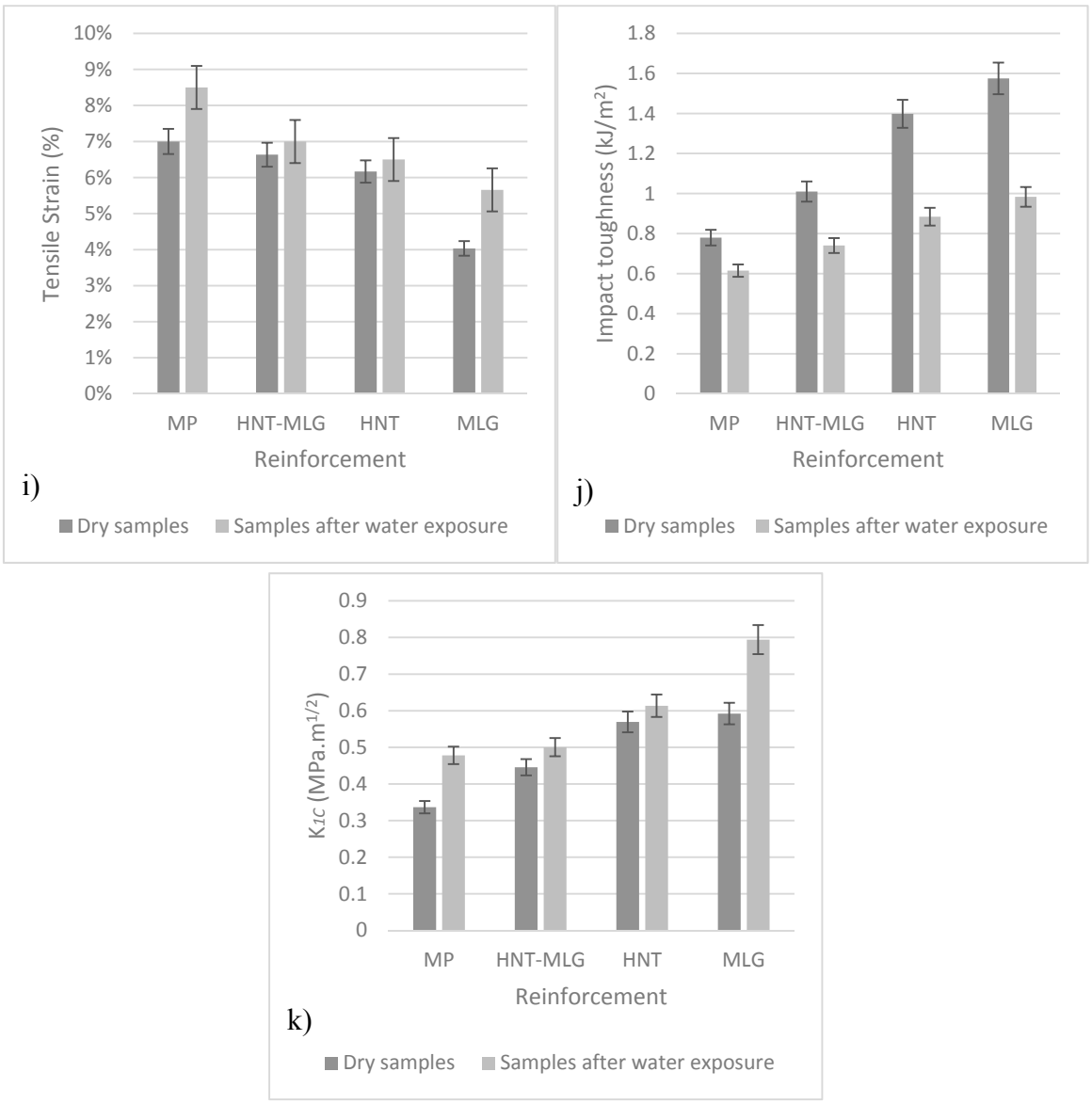

Figure 7. Mechanical properties of nanocomposites in dry condition and after water exposure

5. Topographic profile

The topographical study was carried out on fractured three-point bend samples. The surface roughness (R_a) of monolithic polyester, 0.05 wt% HNT-0.05 wt% MLG. 0.1 wt% HNT and 0.1 wt% MLG are shown in Figure 8. The R_a is defined as the mean of the roughness profile and is superimposed on the surface waviness [40]. The R_a (Figure 8(a)) value for monolithic polyester was 0.32 µm. The R_a then increased steadily for samples reinforced with 0.05 wt% HNT-MLG (0.48 µm), 0.1 wt% HNT (0.68 µm) and 0.1 wt% MLG (0.8 µm). The R_a values for samples exposed in water increased compared to dry condition. The water molecules diffused through the polymer matrix and congregating around the particles [45]. This lead to increase in plastic zone which then increased the surface roughness of the nanocomposites.

The similar trend also observed for R_q and R_z for nanocomposites tested in dry and after water exposure. R_q is the root mean square of the profile and sensitive to surface variation 29. The peak-to-valley heights or R_z measures highest and lowest point of the profile. R_q for 0.1 wt% MLG reinforced polyester in air was 0.71 µm and the R_z was 4.43 µm. After water exposure the maximum R_q and R_z for 0.1 wt% MLG reinforced polyester was 1µm and 5.5 µm. A high value of R_a (with low R_z value) can be on indicator of smoother samples surfaces, absence of agglomerates and uniform dispersion of nano-fillers. A low value of R_a but high R_z value shows the existence of deep surface notches,

agglomerates, and non-uniform dispersion of nano-fillers. In general, R_q (Figure 8 (b)) and R_z (Figure 8(c)) were lower in dry condition and higher after water exposure. After water exposure, coarser topography was observed.

The flexural strain samples (from three point-bend test) used for the surface roughness measurement kept increasing with the coarser topography. This can be attributed to lower stiffness and strength values. A schematic illustration on topography difference between polyester nanocomposites tested in air and after water exposure is illustrated in Figure 9. The topography profile after water exposure became coarser because of plasticization effect. The increase of high peaks can be linked to the water absorption. The topography surface profile of nanocomposites for samples tested in air and wet condition is presented in Figure 10. It can be observed that after water exposure, the surface profiles were coarser than dry samples.

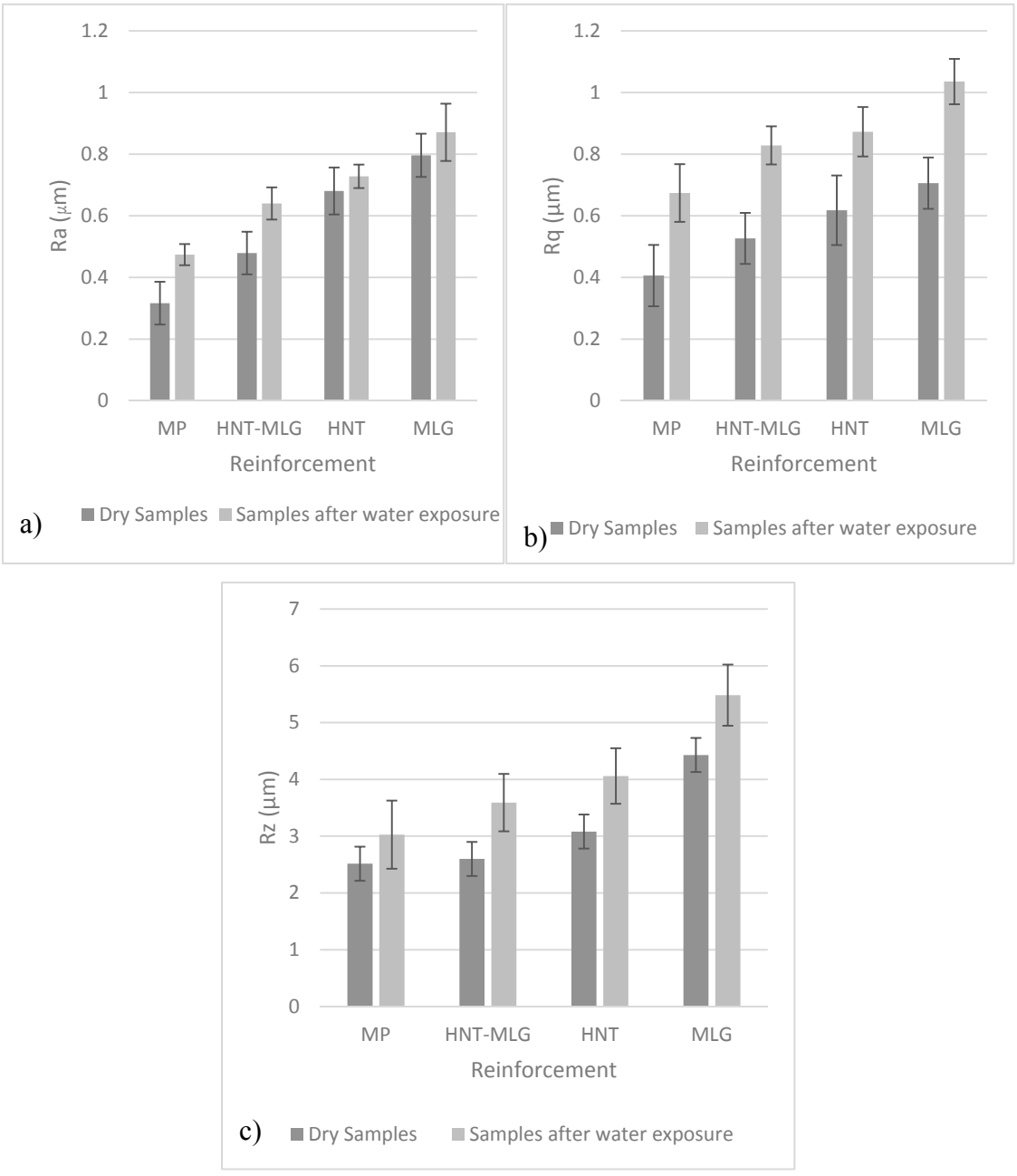

Figure 8. topographic features of nanocomposites in dry condition and after water exposure

Peer-reviewed version available at Polymers 2017, 9, 27; doi:10.3390/polym9010027

Figure 9. Topography profile of samples in dry condition and after water exposure

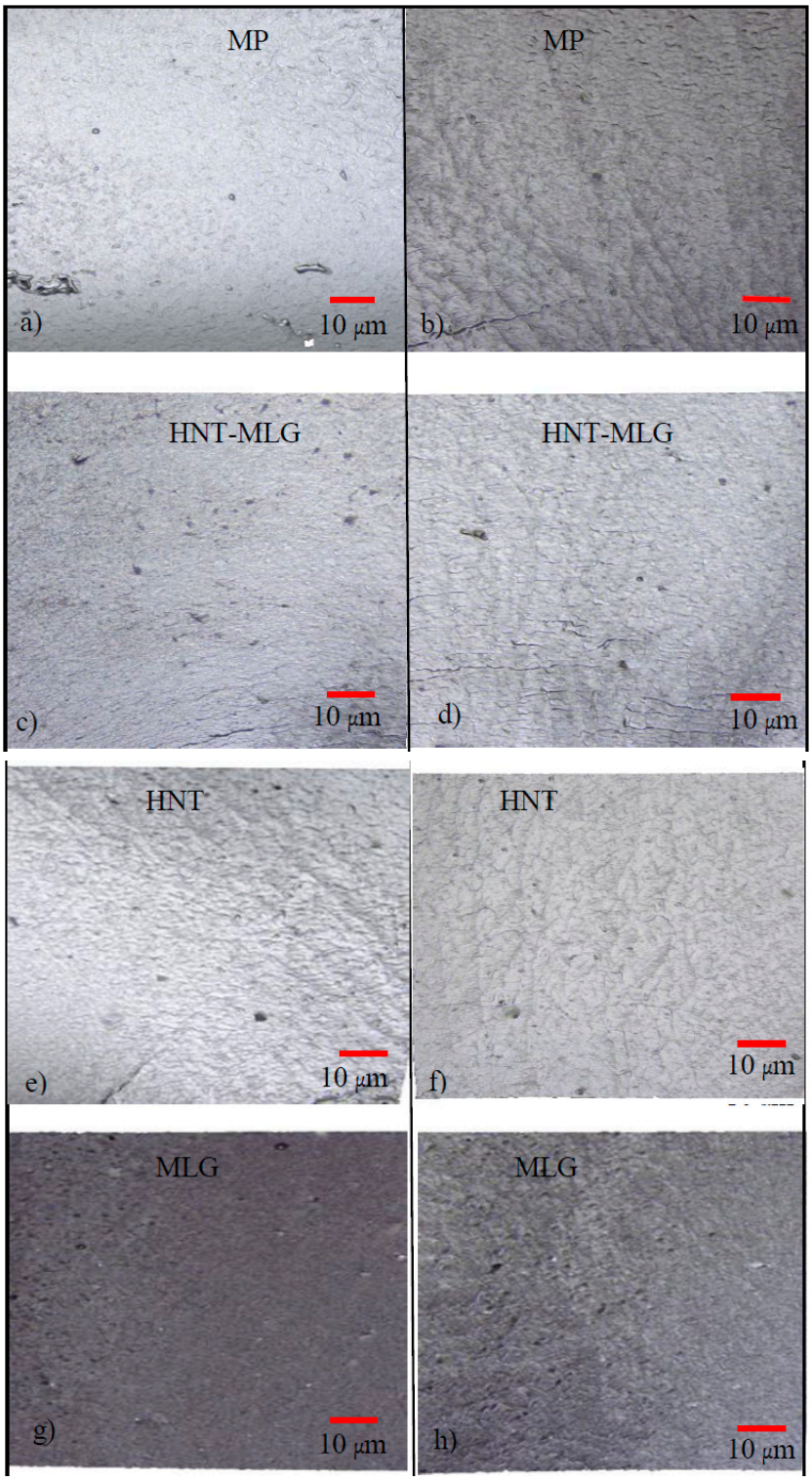

Figure 10. Surface profile of nanocomposites before and after water exposure

Peer-reviewed version available at Polymers 2017, 9, 27; doi:10.3390/polym9010027

6. Fractography

The SEM images of fractured surfaces are shown in Figure below 11. As the cracks propagates, material is lost most likely in the form of round particles as it can be observed in Figure 11 (a). The image also revealed that the monolithic sample was showing river markings which can be associated with fast brittle fracture mode [46]. That is an evident that there are no crack bridging mechanisms available in monolithic polyester. When the cracks propagated, they move with less diversions. After water exposure, the monolithic polyester shows more smooth surface with weaker crack lines can be observed. The de-bonding for MP is in the form of long and straight lines.

Synergistic effects are not effective at concentration of 0.1 wt% to produce considerable improvement in mechanical properties of produced hybrid nanocomposites [47]. De-bonded clusters of fillers from polyester matrix can be seen for hybrid sample (Figure 11(c)). The size of the clusters is relatively small with considerably small spacing. The material in the vicinity of the clusters and the distance between them may not have significant effect in mechanical properties [48].

The effect of MLG was also noticeable on the surface of the 0.05 wt% HNT-0.05 wt% MLG nanocomposites. The crumpled structure of MLG is shown in Figure 11 (d). The effect of water on hybrid nanocomposites suggest that surface roughness was reduced compared to samples tested in dry conditions [49]. De-bonding and pull-out of fillers were observed in hybrid samples, which are responsible for the moderate toughening in Figure 11 (d) [50].

For the HNT samples, the interlocking effect can alter the crack formation mechanism. In Figure 11 (e), the crack started from a defect point and emanated radially. Similar phenomenon has been reported elsewhere [46]. Crack lines are more straight after the HNT reinforced polyester samples were exposed to water. The nanocomposites containing HNT particles showed plasticization effect where the crack propagation became easier and faster.

Graphene based materials are often compliant, and when dispersed in a polymer matrix, they are typically not observed as rigid discs but rather as a bent or crumpled platelets [51]. The wrinkle structure of MLG has better interfacial interactions than the tubular structure of HNT [52]. The wrinkled structure significantly improves the interfacial interactions with the polyester chains. The Figure 11(g) shows no particular crack orientation. This is because MLG has the ability to prevent the propagation of cracks and cracks detour around the MLG to proceed [53]. After water exposure, micro-cracks and pronounced river markings can be observed for the MLG reinforced sample. It is evident that presence of HNT and MLG fillers increased the fracture surface roughness. That is an indicator of crack deflection mechanism, which increases the absorbed energy of fracture by increasing the crack length during deformation [54].

The fracture nature between monolithic polyester, hybrid, HNT and MLG reinforced polyester are different from each other. Lower resistance to crack propagation shows more straight paths and smooth surface. This can be observed in case of monolithic polyester and hybrid nanocomposites. Hybrid nanocomposites showed moderate toughening mechanism but slightly better than unfilled polyester. It can be observed that 0.1 wt% HNT reinforced polyester shows high resistance to crack propagation compared to monolithic polyester and hybrid nanocomposites with round ended cracks. High aspect ratio of MLG, however, showed superior toughening than other nanocomposites system. The force required for crack propagation of 0.1 wt% MLG reinforced polyester was higher based on the SEM images evident.

Results obtained suggested that there was no significant improvement in water barrier properties and mechanical performance in hybrid nanocomposites. This is because 0.05 wt% of HNT and MLG is either not enough to produce significant synergistic effect or there are no synergistic effects between HNT and MLG. Based on SEM images, there was no evidence that HNT and MLG were poorly dispersed. The weight fraction used was only 0.1% and therefore the inferior dispersion state can be ruled out as a cause for the degradation of mechanical properties. It is noted from literature; the diffusion of moisture can be distributed throughout the polymer matrix or be drawn to form water clusters [55]. In this research, the formation of water clusters was not observed in SEM images but plasticization effect was clearly noticed. Therefore, plasticization of matrix is mainly

Peer-reviewed version available at Polymers 2017, 9, 27; doi:10.3390/polym9010027

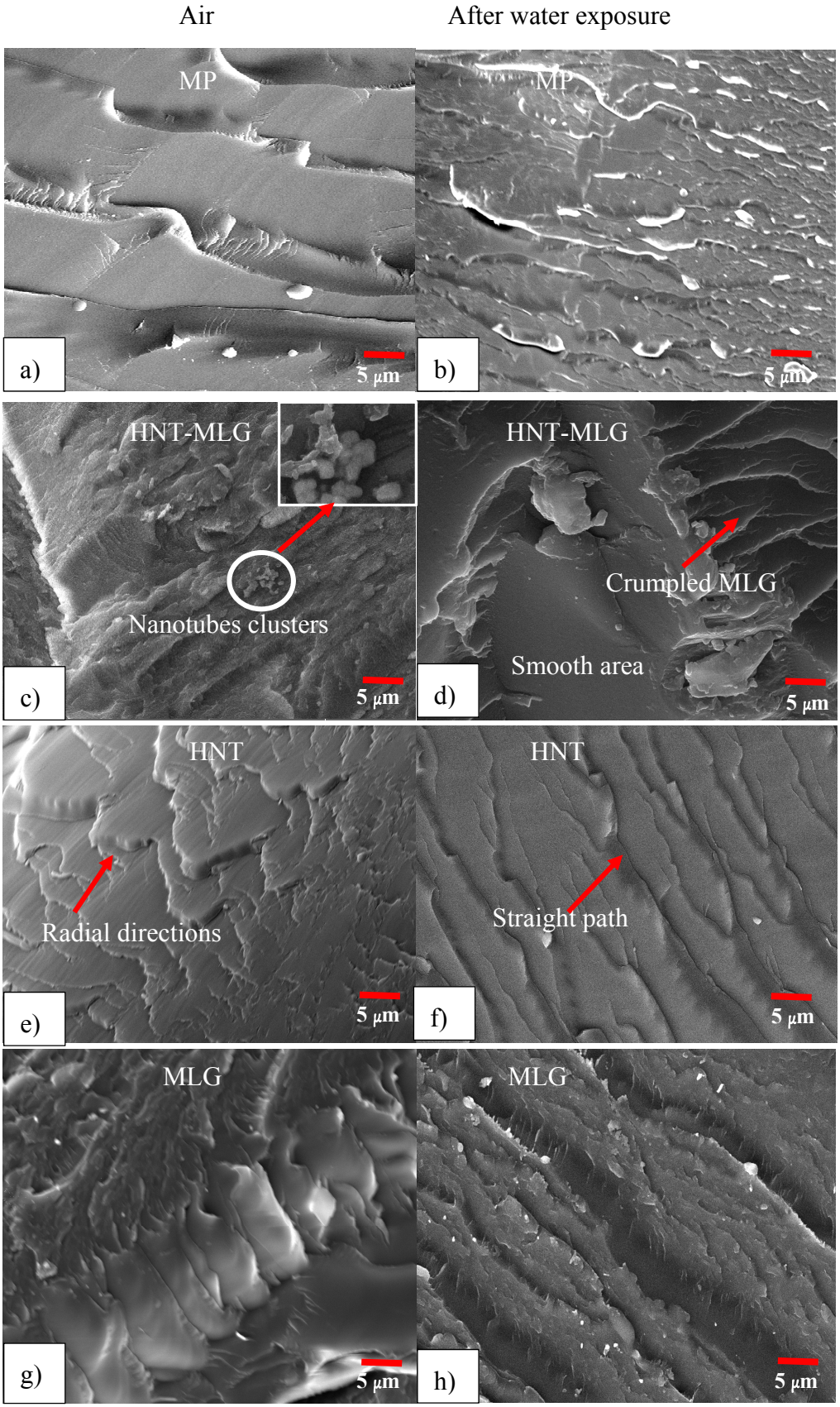

Figure 11. SEM images of nanocomposites before and after water exposure

responsible for the degradation of mechanical properties for all nanocomposites system (MP, HNT-MLG, HNT and MLG reinforced polyesters).

8. Conclusions

The effect of short water absorption with 60 °C temperature on the mechanical properties of HNT (halloysite nanotube) and multi-layer graphene (MLG) reinforced polyester has been studied. It is shown that polyester matrix is vulnerable to water exposure. Addition of small amount of HNT and MLG decreased the weight gain of the nanocomposites compared to monolithic polyester. MLG reinforced polyester showed superior strength compared to hybrid and HNT in dry condition and after water exposure. The SEM images revealed less number of cracks for all samples exposed in water. Nano-filler and matrix interface weakening was the main failure mechanism induced by water exposure. The degradation of mechanical properties related to water absorption caused softening of polymer matrix which lowered the strength of nanocomposites. Fracture toughness of nanocomposites after water exposure increased because of plasticization effect. The surface roughness of all nanocomposites system increased after water exposure. This can be attributed to the high peaks and plasticized crack zone which then produced coarser topography. This study provided evidence that synergistic effect of HNT-MLG hybrid nanocomposites at low content (0.05 wt% HNT-0.05 wt% MLG) was insufficient to produce remarkable mechanical properties in dry condition and after water exposure. More research can be conducted to improve the mechanical properties of hybrid composites exposed to different liquid environment at different temperature.

Acknowledgement

The authors wish to thank Majlis Amanah Rakyat Malaysia (MARA) and Northumbria University for the research funding and facilities provided in this research.

References

1. Saharudin, M. S.; Jumahat, A.; Kahar, A. Z.; Ahmad, S. The Influence of Alumina Filler on Impact Properties of Short Glass Fiber Reinforced Epoxy. In *Applied Mechanics and Materials*; 2013; Vol. 393, pp. 88–93.

2. Saharudin, M. S.; Shyha, I.; Inam, F. The effect of methanol exposure on the flexural and tensile properties of halloysite nanoclay polyester. In *The IRES 17th International Conference, United Kingdom*; London, 2015; pp. 40–44.

3. Saharudin, M. S.; Shyha, I.; Inam, F. Viscoelastic and mechanical properties of multi-layered-graphene polyester composites. In *2nd International Conference on Advances in Mechanical Engineering*; Yildiz Technical University: Istanbul, 2016; pp. 41–45.

4. Ollier, R.; Rodriguez, E.; Alvarez, V. Unsaturated polyester/bentonite nanocomposites: Influence of clay modification on final performance. *Compos. Part A Appl. Sci. Manuf.* **2013**, *48*, 137–143.

5. Bonnia, N. N. Mechanical properties and environmental stress cracking resistance of rubber toughened polyester/kenaf composite. *eXPRESS Polym. Lett.* **2010**, *4*, 55–61.

6. George, J.; Bhagawan, S. S.; Thomas, S. Effects of environment on the properties of low-density polyethylene composites reinforced with pineapple-leaf fibre. *Compos. Sci. Technol.* **1998**, *58*, 1471–1485.

7. Saharudin, M. S.; Atif, R.; Shyha, I.; Inam, F. The degradation of mechanical properties in polymer nano-composites exposed to liquid media – a review. *RSC Adv.* **2016**, *6*, 1076–1089.

8. Akil, H. M.; Santulli, C.; Sarasini, F.; Tirillò, J.; Valente, T. Environmental effects on the mechanical behaviour of pultruded jute/glass fibre-reinforced polyester hybrid composites. *Compos. Sci. Technol.* **2014**, *94*, 62–70.

9. Saharudin, M. S.; Rasheed, A.; Shyha, I.; Inam, F. The degradation of mechanical properties in halloysite nanoclay – polyester nanocomposites exposed to diluted methanol. *J. Compos. Mater.* **2016**, 1–12.

10. Joseph, P. .; Rabello, M. S.; Mattoso, L. H. .; Joseph, K.; Thomas, S. Environmental effects on the degradation behaviour of sisal fibre reinforced polypropylene composites. *Compos. Sci. Technol.* **2002**, *62*, 1357–1372.

11. Mazuki, A. A. M.; Akil, H. M.; Safiee, S.; Ishak, Z. A. M.; Bakar, A. A. Degradation of dynamic mechanical properties of pultruded kenaf fiber reinforced composites after immersion in various solutions. *Compos. Part B Eng.* **2011**, *42*, 71–76.

12. Gao, F. Clay/polymer composites: the story. *Mater. Today* **2004**, *7*, 50–55.

13. Saharudin, M. S.; Atif, R.; Shyha, I.; Inam, F. The degradation of mechanical properties in halloysite nanoclay-polyester nanocomposites exposed to diluted methanol. *J. Compos. Mater.* **2016**, 0021998316660178.

14. Gilman, J. W. Flammability and thermal stability studies of polymer layered-silicate (clay) nanocomposites. *Appl. Clay Sci.* **1999**, *15*, 31–49.

15. Gilman, J. W.; Kashiwagi, T.; Lichtenhan, J. D. Nanocomposites: A revolutionary new flame retardant approach. *SAMPE J.* **1997**, *33*, 40–46.

16. Müller, C. M. O.; Laurindo, J. B.; Yamashita, F. Effect of nanoclay incorporation method on mechanical and water vapor barrier properties of starch-based films. *Ind. Crops Prod.* **2011**, *33*, 605–610.

17. Lewis, P. R. Environmental stress cracking of polycarbonate catheter connectors. *Eng. Fail. Anal.* **2009**, *16*, 1816–1824.

18. Robeson, L. M. Environmental stress cracking: A review. *Polym. Eng. Sci.* **2013**, *53*, 453–467.

19. Alamri, H.; Low, I. M. Effect of water absorption on the mechanical properties of nano-filler reinforced epoxy nanocomposites. *Mater. Des.* **2012**, *42*, 214–222.

20. Das, T. K.; Prusty, S. Graphene-Based Polymer Composites and Their Applications. *Polym. Plast. Technol. Eng.* **2013**, *52*, 130227104444003.

21. Geim, A. K.; Novoselov, K. S. The rise of graphene. *Nat. Mater.* **2007**, *6*, 183–191.

22. Balandin, A. A.; Ghosh, S.; Bao, W.; Calizo, I.; Teweldebrhan, D.; Miao, F.; Lau, C. N. Superior thermal conductivity of single-layer graphene. *Nano Lett.* **2008**, *8*, 902–907.

23. Novoselov, K. S.; Fal'ko, V. I.; Colombo, L.; Gellert, P. R.; Schwab, M. G.; Kim, K. A roadmap for graphene. *Nature* **2012**, *490*, 192–200.

24. Atif, R.; Wei, J.; Shyha, I.; Inam, F. Use of morphological features of carbonaceous materials for improved mechanical properties of epoxy nanocomposites. *RSC Adv.* **2016**, *6*, 1351–1359.

25. Atif, R.; Inam, F. Influence of macro-topography on mechanical performance of 0.5 wt% nanoclay/multi-layer graphene-epoxy nanocomposites. *AIMS Mater. Sci.* **2016**, *3*, 1294–1308.

26. Atif, R.; Shyha, I.; Inam, F. The degradation of mechanical properties due to stress concentration caused by retained acetone in epoxy nanocomposites. *RSC Adv.* **2016**, *6*, 34188–34197.

27. Atif, R.; Inam, F. Influence of Macro-Topography on Damage Tolerance and Fracture Toughness of Multi-Layer Graphene/Clay-Epoxy Nanocomposites. **2016**, 335–360.

28. Ratna Prasad, A. V.; Mohana Rao, K. Mechanical properties of natural fibre reinforced polyester composites: Jowar, sisal and bamboo. *Mater. Des.* **2011**, *32*, 4658–4663.

29. Ye, Y.; Chen, H.; Wu, J.; Ye, L. High impact strength epoxy nanocomposites with natural nanotubes. *Polymer (Guildf).* **2007**, *48*, 6426–6433.

30. Preghenella, M.; Pegoretti, A.; Migliaresi, C. Thermo-mechanical characterization of fumed silica-epoxy nanocomposites. *Polymer (Guildf).* **2005**, *46*, 12065–12072.

31. Nair, R. R.; Wu, H. a.; Jayaram, P. N.; Grigorieva, I. V.; Geim, a. K. Unimpeded Permeation of Water Through Helium-Leak-Tight Graphene-Based Membranes. *Science (80-.).* **2012**, *335*, 442–444.

32. John, B.; Nair, C. P. R.; Ninan, K. N. Effect of nanoclay on the mechanical, dynamic mechanical and thermal properties of cyanate ester syntactic foams. *Mater. Sci. Eng. A* **2010**, *527*, 5435–5443.

33. Zainuddin, S.; Hosur, M. V.; Zhou, Y.; Kumar, A.; Jeelani, S. Durability studies of montmorillonite clay filled epoxy composites under different environmental conditions. *Mater. Sci. Eng. A* **2009**, *507*, 117–123.

34. Bastiurea, M.; Rodeanu, M. S.; Dima, D.; Murarescu, M.; Andrei, G. Thermal and Mechanical Properties of Polyester Composites With Graphene Oxide and Graphite. *Dig. J. Nanomater. Biostructures* **2015**, *10*, 521–533.

35. Gabr, M. H.; Phong, N. T.; Abdelkareem, M. A.; Okubo, K.; Uzawa, K.; Kimpara, I.; Fujii, T. Mechanical, thermal, and moisture absorption properties of nano-clay reinforced nano-cellulose biocomposites. *Cellulose* **2013**, *20*, 819–826.

36. Huang, G.; Sun, H. Effect of water absorption on the mechanical properties of glass/polyester composites. *Mater. Des.* **2007**, *28*, 1647–1650.

37. Saharudin, M.; Wei, J.; Shyha, I.; Inam, F. The degradation of mechanical properties in halloysite nanoclay-polyester nanocomposites exposed in seawater environment. *J. Nanomater.* **2016**.

38. Maharsia, R.; Gupta, N.; Jerro, H. D. Investigation of flexural strength properties of rubber and nanoclay reinforced hybrid syntactic foams. *Mater. Sci. Eng. A* **2006**, *417*, 249–258.

39. Atif, R.; Shyha, I.; Inam, F. Mechanical, Thermal, and Electrical Properties of Graphene-Epoxy Nanocomposites—A Review. *Polymers (Basel).* **2016**, *8*, 281.

40. Atif, R.; Inam, F. Influence of macro-topography on damage tolerance and fracture toughness of 0.1 wt % multi-layer graphene/clay-epoxy nanocomposites. *Polymers (Basel).* **2016**, *8*.

41. Hough, M. C.; Wright, D. C. Two new test methods for assessing environmental stress cracking of amorphous thermoplastics. *Polym. Test.* **1996**, *15*, 407–421.

42. Hojo, H.; Ogasawara, K.; Chang, W. .; Tsuda, K. Degradation behavior of unsaturated polyester resin in alcohols. *Adv. Compos. Mater.* **1994**, *3*, 341–353.

43. Dhakal, H.; Zhang, Z.; Richardson, M. Effect of water absorption on the mechanical properties of hemp fibre reinforced unsaturated polyester composites. *Compos. Sci. Technol.* **2007**, *67*, 1674–1683.

44. Indrani, D. J.; Cook, W. D.; Televantos, F.; Tyas, M. J.; Harcourt, J. K. Fracture toughness of water-aged resin composite restorative materials. *Dent. Mater.* **1995**, *11*, 201–207.

45. Sancaktar, E.; Kuznicki, J. Nanocomposite adhesives: Mechanical behavior with nanoclay. *Int. J. Adhes. Adhes.* **2011**, *31*, 286–300.

46. Vahedi, V.; Pasbakhsh, P. Instrumented impact properties and fracture behaviour of epoxy/modified halloysite nanocomposites. *Polym. Test.* **2014**, *39*, 101–114.

47. Peeterbroeck, S.; Alexandre, M.; Nagy, J. B.; Pirlot, C.; Fonseca, A.; Moreau, N.; Philippin, G.; Delhalle, J.; Mekhalif, Z.; Sporken, R.; Beyer, G.; Dubois, P. Polymer-layered silicate–carbon nanotube nanocomposites: unique nanofiller synergistic effect. *Compos. Sci. Technol.* **2004**, *64*, 2317–2323.

48. Liu, W.; Hoa, S. V.; Pugh, M. Water uptake of epoxy-clay nanocomposites: Model development. *Compos. Sci. Technol.* **2008**, *68*, 156–163.

49. Rothon, R. *Particulate-Filled Polymer Composites*; 2003.

50. Zeng, Y.; Liu, H.-Y.; Mai, Y.-W.; Du, X.-S. Improving interlaminar fracture toughness of carbon fibre/epoxy laminates by incorporation of nano-particles. *Compos. Part B Eng.* **2012**, *43*, 90–94.

51. Potts, J. R.; Dreyer, D. R.; Bielawski, C. W.; Ruoff, R. S. Graphene-based polymer nanocomposites. *Polymer (Guildf).* **2011**, *52*, 5–25.

52. Stankovich, S.; Dikin, D. a; Dommett, G. H. B.; Kohlhaas, K. M.; Zimney, E. J.; Stach, E. a; Piner, R. D.; Nguyen, S. T.; Ruoff, R. S. Graphene-based composite materials. *Nature* **2006**, *442*, 282–286.

53. Feng, H.; Wang, X.; Wu, D. Fabrication of spirocyclic phosphazene epoxy-based nanocomposites with graphene via exfoliation of graphite platelets and thermal curing for enhancement of mechanical and conductive properties. *Ind. Eng. Chem. Res.* **2013**, *52*, 10160–10171.

54. Bhattacharya, M. Polymer nanocomposites-A comparison between carbon nanotubes, graphene, and clay as nanofillers. *Materials (Basel).* **2016**, *9*, 1–35.

55. Moghbelli, E.; Banyay, R.; Sue, H. J. Effect of moisture exposure on scratch resistance of PMMA. *Tribol. Int.* **2014**, *69*, 46–51.